Supporting Material

Elevated methylmercury production in mercury-contaminated soil and its bioaccumulation in rice: key roles of algal decomposition

Di Liu[1,2,3], Yan Wang[1,2,3], Tianrong He[1], Deliang Yin (✉)[1], Shouyang He[1], Xian Zhou[1,2,3], Yiyuan Xu[2], Enxin Liu[1,2,3]

1 Key Laboratory of Karst Georesources and Environment (Ministry of Education), Guizhou University, Guiyang 550025, China
2 College of Resources and Environmental Engineering, Guizhou University, Guiyang 550025, China
3 Guizhou Karst Environmental Ecosystems Observation and Research Station, Ministry of Education, Guiyang 550025, China

Text S1

Measurement of DOM concentration and properties

Soil DOC concentrations in the SDOM filtrates were quantified using a TOC analyzer (Vario TOC, Elementar, Germany).

The cysteine-containing SDOM filtrates were first concentrated to approximately 2 mL at 50 ℃ under vacuum conditions (0.08 MPa), and the cysteine concentrations were then detected by high-performance liquid chromatography (flow phase was a mixed liquor of 10% methanol and 0.1% phosphate). The detailed procedures can be accessed in a previous report by Lu et al.(Lu, 2020).

The SDOM filtrates used for measuring the Fourier transform infrared (FTIR) spectroscopy were first vacuum-freeze dried at -60 ℃. The FTIR of solid SDOM was then characterized by a Fourier transform infrared spectrometer (Nicolet 6700, Thermo Fisher, America) with a scanning range of 4000-400 cm^{-1} and a resolution of 0.4 cm^{-1}. Several relative spectral parameters can be found in **Table S2.**

✉Corresponding author
E-mail: dlyin@gzu.edu.cn

Nuclear magnetic resonance (NMR) spectroscopy can help us understand the molecular composition of SDOM, such as functional groups. The SDOM filtrates used for measuring nuclear magnetic resonance (NMR) spectroscopy were first vacuum-freeze dried at -60 ℃. To achieve ^{13}C nuclear magnetic resonance spectroscopy of SDOM, approximately 200 mg of a solid SDOM sample was filled into a 4 mm double resonance probe and was then measured using a solid-state NMR spectrometer (AVANCE NEO 400WB, Bruker, Germany) featuring a set of operating parameters, including spectral frequency (100.6 MHz), spinning rate (8 kHz), cross-polarization time (1.5 ms), data acquisition time (0.01 s), delay time (1 s), pulse width (4.5 μs), cross-polarization time (1 μs) and scan spectrum width (300 PPM).

Ultraviolet-visible (UV-Vis) and fluorescent spectroscopies of filtrates were measured using an Aqualog fluorescence spectrophotometer equipped with a 150 W ozone-free xenon lamp at a constant 20 ℃ (Aqualog, Horiba, Japan). Milli-Q deionized water was used as the blank to remove the interferences of water Raman peaks, and Aqualog data-processing software automatically corrected Rayleigh and Raman scatterings. The detailed procedures were reported by Jiang et al.(Jiang et al., 2018), and the relative spectral parameters can be found in **Table S3**. Briefly, the a(355) represents the colored DOM (CDOM), which is the part of DOM that absorbs blue light, determining physical and chemical conditions in freshwaters (Helms et al., 2009); $SUVA_{254}$ reflects the DOM aromaticity, the higher $SUVA_{254}$ value, the higher DOM aromaticity (Weishaar et al., 2003); S_R reflects the DOM molecular weight, the lower S_R value, the higher DOM molecular weight (Helms et al., 2009); and Humification index (HIX) reflects the DOM humification level, the higher HIX value, the higher humification level (Ohno, 2002).

TEXT S2

DNA sequencing

DNA sequencing methods were mainly followed by a previous report, and slightly modified (Xiang et al., 2018). The PCR reactions were performed in a 20 μL volume using an ABI PCR instrument (GenenAmp® 9700), containing 4 μL 5 × FastPfu buffer, 2 μL dNTPs (2.5 mmol L^{-1}), 0.8 μL forward primer (5 μM), 0.8 μL reverse primer (5 μM), 0.4 μL FastPfu polymer (TransStart Fastpfu DNA polymerase, TransGen AP221-02), 0.2 μL BSA, and 10 ng template DNA. The amplification condition was as follows: 1) initial denaturation at 95 ℃ for 3 min; 2) 27 cycles of denaturation at 95 ℃ for 30 sec, annealing at 55 ℃ for 30 sec, and extension at 72 ℃ for 45 sec; and 3) final elongation at 72 ℃ for 10 min, and then cooling to 10 ℃ until halted by user. Triplicates were run with each sample. The the PCR products were then recovered by A xyPrepDNA Gel Extration Kit (Axygen Bio, USA), while were eluted by Tris_HCL. After that, the PCR products from the same sample were pooled, and analyzed with 3 μL of the product on a 2% agarose gel electrophoresis. According to the result from gel electrophoresis, the PCR products were quantified using a QuantiFluor™-ST Fluorometer (Promega (Beijing) Biotech Co., Ltd, China), and mixed into appropriate proportions. After that, the prepared samples were sequenced with Miseq PE300 platform (Illumina, America) in the Majorbio Biopharm Technology Co., Ltd (Shanghai, China).

TEXT S3

PARAFAC was calculated using two- to seven-component models with non-negative constraints, after which the number of fluorescent components was determined by residual analysis, split-half analysis, and visual examination (Huang et al., 2018). After the PARAFAC model was established, fluorescent component species in SDOM samples were compared with the literature database in the efc software via Tucker congruence coefficients (TCC). Such an operation provides an analogy to find similar component fingerprints. In this study, the PARAFAC method picked out two fluorescent components from SDOM at different 3D-EEM spectra, i.e., humic-like components (C1, C2, and C3) and a protein-like component (C4). After comparing, humic-like C1 is possibly derived

from anthropogenic sources such as animal manure fertilizers, humic-like C2 is related to microbial organic synthesis, humic-like C3 is mainly composed of high-molecular-weight or aromatic compounds, and protein-like C4 is a tyrosine-like amino acid representing degraded peptide materials (Stedmon and Markager, 2005; Fellman et al., 2009; Kowalczuk et al., 2010; Yamashita et al., 2010).

Table S1 Initial elemental contents of experimental materials

Materials	THg (ng g^{-1})	MeHg (ng g^{-1})	N (%)	C (%)	H (%)	S (%)	C/N	H/C
Soil	5210.00	1.22	0.29	2.75	0.94	0.29	9.48	0.34
Algae	45.24	2.28	3.81	34.29	4.79	1.84	9.00	0.14

Table S2 Major adsorption bands of FTIR spectroscopy in soil DOM amended by algal biomass (15 g)

Wavenumber (cm^{-1})	Descriptions	References
3500-3000	Hydrogen bonded O-H stretching in alcohols and residual water	(Beratto et al., 2017)
2354	Antisymmetric stretching vibration of CO_2	(Wang et al., 2011)
1644-1618	Amide I, antisymmetric stretching C=O peptide bond, H-O-H bending in water, Antisymmetric stretching of COO-	(Beratto et al., 2017) (Wu et al., 2004)
1415	Lignin and aliphatic compounds in the double bond or carbonyl connected - CH_2 deformation vibration and inorganic NH^{4+}, NO^{3-} and organic carboxylate COO- absorption	(Wu et al., 2004; Wang et al., 2011)
1133	Polysaccharides, C-O-C stretching	(Beratto et al., 2017)
869	CO_3^{2-}	(Wang et al., 2011)
673	Characteristic peaks of aromatic ring class	(Wang et al., 2011)
597	Inside-out variable angle vibration of hydroxyl	(Wu et al., 2004)

Table S3 Ultraviolet-visible and fluorescent spectrum indices

Spectral parameters	Calculation method	Descriptions	References
a(355)	$a(\lambda)=2.303D(\lambda)/L$, $a(\lambda)$ is the absorption coefficient at wavelength λ(nm), $D(\lambda)$ is the absorbance at a wavelength λ(nm), L is the cuvette path (m)	It represents the concentration of chromophoric DOM (CDOM), which increases with the value. It is the light-absorbing fraction of DOM.	(Helms et al., 2009)
$SUVA_{254}$	$SUVA_{254}=a(254)/DOC$, a(254) is the absorption coefficient at wavelength 254 nm, DOC is dissolved organic carbon (mg L^{-1})	Indicator of DOM aromaticity, which increases with the $SUVA_{254}$ value.	(Weishaar et al., 2003)
Humification index (HIX)	The area under the emission wavelength (Em) 435-480 nm divided by the peak area (300-345 nm + 435-480) nm, at emission wavelength (Em) 254 nm.	Indicator of humic substance content or extent of humification. Higher values indicate an increasing degree of humification.	(Ohno, 2002)
Spectral slope ratio (S_R)	$S_R=S(275\text{-}295)/S(350\text{-}400)$, S is slope of absorption spectrum curve. S(275-295) and S(350-400) are the S values at wavelength 275-295 nm and 350-400 nm, respectively.	Related to DOM molecular weight. Higher S_R values indicate a decreasing molecular weight and aromaticity of DOM.	(Helms et al., 2009)

Table S4 Diversity indices of bacteria in the “control” and “algae” treatments (A_{15} = algal treatments with 15 g biomass)

Rice-growing stages	Treatments	Ace	Chao	Shannon	Coverage
Tillering stage	Control	4977.46	4916.67	6.58	0.9880
	A_{15}	5957.96	5861.82	7.02	0.9832
Filling stage	Control	5971.43	5842.21	6.90	0.9847
	A_{15}	5073.76	5027.90	6.15	0.9806
Mature stage	Control	4986.90	4918.53	6.66	0.9748
	A_{15}	4855.22	4771.14	6.56	0.9814

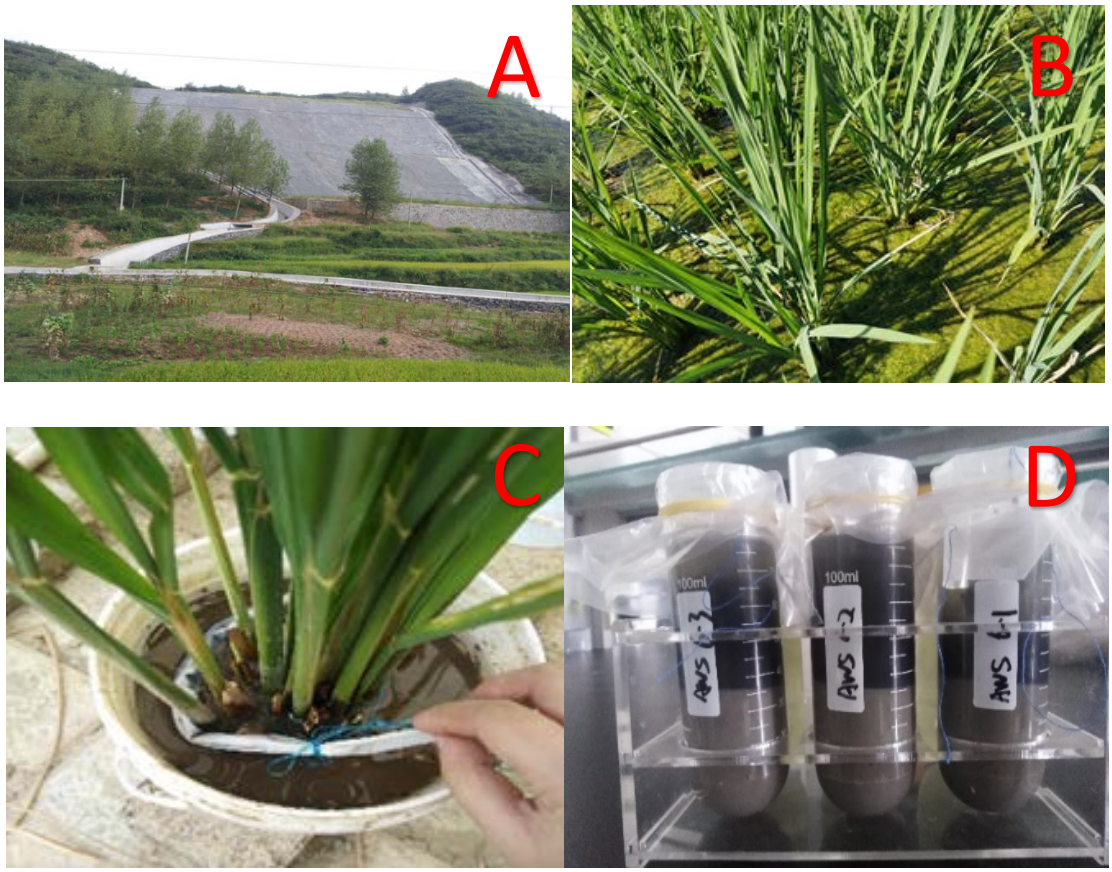

Fig. S1. Photos of research background and experiments (graph A, historical Hg mine in Wanshan; graph B, algal blooms in Hg-mining paddy fields; graph C, pot experiment; graph D, microcosm experiment)

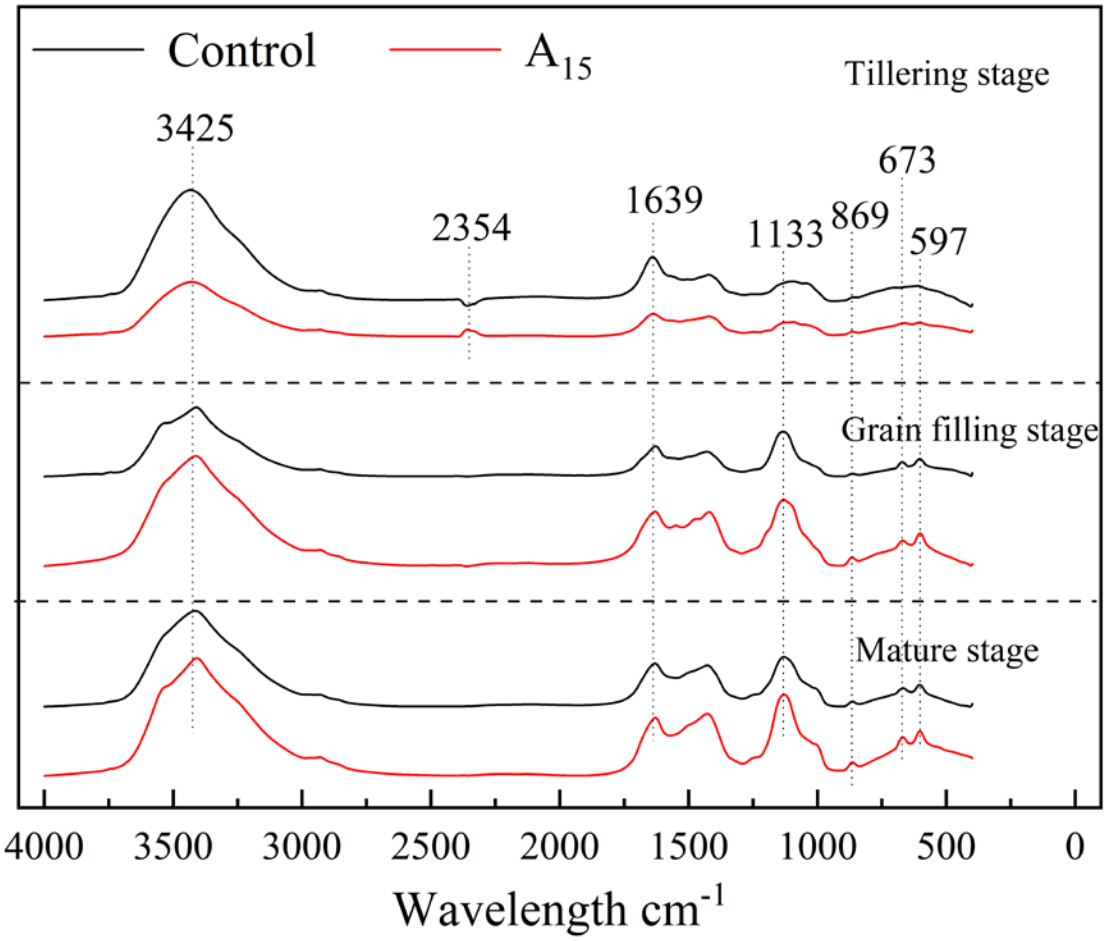

Fig. S2. FTIR spectroscopy of soil DOM regulated by algal decomposition (A_{15} = Algal treatments with 15 g biomass)

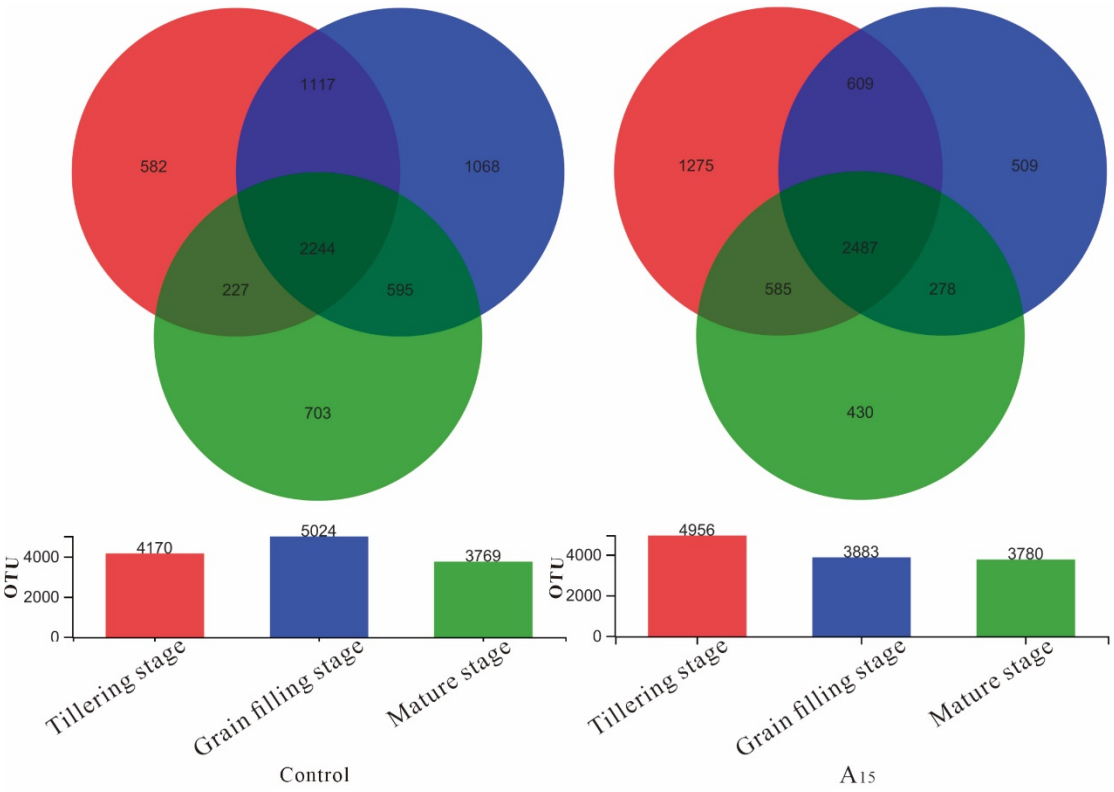

Fig. S3 Venn diagrams of the microbial community at OUT level regulated by algal decomposition (A_{15} = Algal treatments with 15 g biomass)

References:

Beratto A, Agurto C, Freer J, Peña-Farfal C, Troncoso N, Agurto A, Castillo R D P (2017). Chemical Characterization and Determination of the Anti-Oxidant Capacity of Two Brown Algae with Respect to Sampling Season and Morphological Structures Using Infrared Spectroscopy and Multivariate Analyses. Appl Spectrosc, 71(10): 2263-2277

Helms J R, Stubbins A, Ritchie J D, Minor E C, Kieber D J, Mopper K (2009). Absorption spectral slopes and slope ratios as indicators of molecular weight, source, and photobleaching of chromophoric dissolved organic matter. Limnology and Oceanography, 54(3): 1023-1023

Huang M, Li Z, Huang B, Luo N, Zhang Q, Zhai X, Zeng G (2018). Investigating binding characteristics of cadmium and copper to DOM derived from compost and rice straw using EEM-PARAFAC combined with two-dimensional

FTIR correlation analyses. Journal of Hazardous Materials, 344(FEB.15): 539-548

Jiang T, Bravo A G, Skyllberg U, Bjorn E, Wang D, Yan H, Green N W (2018). Influence of dissolved organic matter (DOM) characteristics on dissolved mercury (Hg) species composition in sediment porewater of lakes from southwest China. Water Research, 146: 146-158

Lu L, Zhou, Y, Huang, Z, Liu, C, Zheng, F, Niu, C, Wang, J, Ma, Y, Li, Q, Wang, D (2020). Simultaneous determination of alliin, deoxyalliin and γ-glutamyl-L-cysteine in black garlic by HPLC (in Chinese with English abstract). Journal of Northeast Agricultural University, 51(7): 36-43

Ohno T (2002). Fluorescence inner-filtering correction for determining the humification index of dissolved organic matter. Environmental Science and Technology, 36(4): 742-746

Wang W, Zhao X, Luo Y, Shi C, Ma H, Yu X, Jia H (2011). Infrared spectral analysis during fermentation of cattle manure %J China Cattle Science. 37(02): 15-19

Weishaar J L, Aiken G R, Bergamaschi B A, Fram M S, Fujii R, Mopper K (2003). Evaluation of specific ultraviolet absorbance as an indicator of the chemical composition and reactivity of dissolved organic carbon. Environmental Science and Technology, 37(20): 4702-4708

Wu J, Lv Y, Wang M, Jiang Y (2004). Study on decomposition of organic fertilizers by FTIR %J Plant Nutrition and Fertilizer Science. (03): 259-266

Xiang Y, Wang Y, Zhang C, Shen H, Wang D (2018). Water level fluctuations influence microbial communities and mercury methylation in soils in the Three Gorges Reservoir, China. Journal of Environmental Sciences, 68: 206-217